TOWARDS ASSEMBLING A MATRIX HYBRID COMPOSITE AIRCRAFT SIDE SHELL USING INTERDIFFUSION JOINING

Manuel Endrass*, Ali Kadinoglu, Stefan Jarka, Philipp Gänswürger and Lars Larsen
German Aerospace Center (DLR), Center for Lightweight Production Technology,
Am Technologiezentrum 4
D-86159 Augsburg
*Corresponding author: manuel.endrass@dlr.de

ABSTRACT

Hybrid airframe structures that combine thermoset (TSC) and thermoplastic (TPC) carbon-fiber composites promise lightweight, high-performance components amenable to high-rate production. However, the combination of TSC and TPC poses some challenges for component assembly when conventional joining technologies, such as bolting or adhesive bonding, are to be replaced by material-compatible, high-rate alternatives. This study investigates Assembly Inter-Diffusion Joining (AIDJ), an out-of-autoclave, low-temperature interdiffusion process, for the frame-to-skin joint of the HERFUSE lateral fuselage panel. Three laminate configurations were fabricated: (i) HexPly® 8552 / Ultem™ 1000B (TSC/PEI), (ii) Cetex® TC1225 / Ultem™ 1000B (TPC/PEI), and (iii) a full matrix-hybrid stack replicating the actual joint. Specimens were consolidated under industry-relevant pressure-temperature cycles, inspected with water-coupled ultrasonic testing, and evaluated by slotted single-lap shear and apparent interlaminar shear strength tests. Reflected-light microscopy confirmed a continuous, undisturbed polymer interphase. The results demonstrate that low-temperature interdiffusion joining provides reliable bonds for matrix-hybrid aerospace structures, enabling scalable production and supporting economic objectives.

1. INTRODUCTION

Capabilities for performant, cost efficient and high-rate composite manufacturing play a key role for technology selection within the next generation single-aisle aircraft. Within the air fleets metallic parts are stepwise replaced by either carbonfiber-reinforced polymers (CFRP`s) or in some cases 3D printed parts. New materials and technologies for the manufacturing of CFRP`s are continuously developed and matured according to the market needs. Within one of the latest Clean Aviation (CA) projects - the Multifunctional Fuselage Demonstrator (MFFD) - an all-thermoplastic composite fuselage barrel was manufactured in collaboration of a European consortium demonstrating disruptive and efficient technologies as well as automation approaches for the high-rate composite fuselage manufacturing and assembly [1]. Here, technological potentials were identified and will stepwise strive the path towards implementation. Thermoforming of thermoplastic frames is one of the examples for efficient high-rate manufacturing technologies and bottleneck within a pursued series production. Combining the state-of-the-art composite fuselage skin production made from thermosets, with thermoplastic frames addresses the question with respect to straight forward and material compatible joining processes. Within the CA project HERFUSE – being acronym for Hybrid Electrical Regional Fuselage and Empennage – a lateral fuselage panel will be manufactured from a TSC-TPC (Hexcel HexPly® 8552/IM7 - Toray Cetex® TC1225/T700) matrix mix as one of the project demonstrators. Here, single part manufacturing technologies and joining

technologies for matrix hybrid CFRP`s are addressed and will continuously be elaborated and matured showcasing possible alternatives or supporting the performance of conventional bolted joints.

2. TARGET APPLICATION & CHALLENGES

2.1 HERFUSE Hybrid Lateral Panel Demonstrator

For the manufacturing of the hybrid lateral panel demonstrator within the HERFUSE project the stringers and the skin laminate are manufactured from a Hexcel HexPly® 8552/IM7 thermoset prepreg. Frames and cleats are thermoformed from thermoplastic Toray Cetex® TC1225 CF/LM-PAEK.

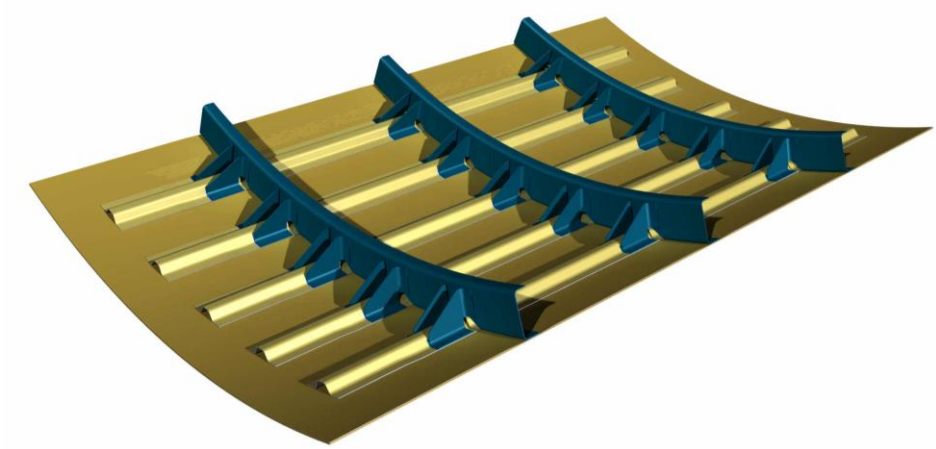


Figure 1 Isometric view of the hybrid lateral panel demonstrator highlighting the individual parts manufactured from thermoset (yellow) and thermoplastic (blue) CFRP`s.

Both material systems have either been extensively studied in aerospace research or tested in flight operations and show preferential capabilities with respect to mechanical performance and streamlined single part manufacturing. The assembly of matrix-hybrid CRFP`s as the next step in the production chain presents challenges when alternatives to conventional bolting technologies are pursued. The combination of neat Hexcel HexPly® 8552/IM7 and Toray Cetex® TC1225/T700 doesn`t intrinsically promote for e.g. joining by thermoplastic welding, whilst conventional adhesive bonding overcomes with an intense pretreatment necessity for thermoset composites and limited adhesion capabilities on semi-crystalline high-performance thermoplastics.

2.2 Processing Requirements and Limitations

Straight forward and industrialized component manufacturing can be achieved by autoclave curing for both, TSC and TPC components. However, for streamlined frame production thermoforming of TPC`s allows to meet the necessary high-rate capability. Neglecting for the present the chemical compatibility and possible miscibility of the individual matrices of the individual components, solutions need to be found, focusing on reliable single part production and material compatible joining. A glance at the processing conditions of the TSC and TPC components (c.f. Table 1) offers a most obvious processing discrepancy for the recommended processing temperature T_P in which the individual parts are cured or consolidated, respectively.

Table 1 Recommended processing parameters for autoclave curing of Hexcel HexPly® 8552 (monolithic parts) and static press consolidation of Toray Cetex® TC1225 with representative values for the respective degradation onset.

	Hexcel HexPly® 8552		Toray Cetex® TC1225	
Processing Temperature T_P [°C]	180°C ± 5 (maximum)	[2]	340– 385, (365 - 395)	[3], ([4])
Processing Pressure p_P [MPa]	0.72	[2]	1.0 – 2.0	[4]
Dwell t_D at T_P [minutes]	120 ± 5	[2]	30 (minimum)	[4]
Degradation Onset (air) $T_{d,onset,O}$ [°C]	242*	[5]	440†	[6]
Degradation Onset* (nitrogen) $T_{d,onset,N}$ [°C]	305	[5]	550 (562.93)	[7], ([8])

Since thermoplastic matrices are usually processed in good approximation at T_m +40 °C, even the degradation onset in nitrogen $T_{d,onset,N}$ is exceeded, when applying conventional fusion bonding technologies. Though, a straight forward joining method must be elaborated, enabling a sufficient structural performance, whilst preventing from thermal degradation.

2.3 Component Modification Approaches to Promote for Hybrid Joining

One first step towards the extension of the portfolio of material compatible and applicable joining technologies could be the local blending of at least the thermoset component using an amorphous polymer film, such as Polyetherimide (PEI) at the common joining interface. The interphase formation mechanisms of Ultem™ 1000B [9] thermoplastic films, co-cured in combination with different TSC`s have been widely investigated preferentially over the last decade [10–19]. Bruckbauer [17] demonstrated, that RTM6-CF-NCF as well as M18/1-CF-UD with PEI or PES modification of the bondline outperform the mechanical performance of the neat thermoset reference, tested for tensile lap shear strength, Mode I and Mode II fracture toughness due to the toughness modification. Thus, meaning a functionalization of the thermoset component is not exclusively preferential for later joining operations, but can also enhance the structural performance of the entire joint. From a joining perspective, the thermoplastic surface modification of the thermoset component intrinsically allows for thermal joining, e.g. ultrasonic, resistance or induction welding. But, thermal degradation of the thermoset component becomes an issue at elevated temperature where conventional high-performance thermoplastics are processed during welding [5,20].

Smiley et al. [21] introduced the thermabond process, demonstrating a reduced-temperature fusion bonding process for the combination of APC2/PES and APC2/PEI. Entirely, it has been shown that the circumstance of bringing both thermoplastic matrices into the melt viscous regime remains necessary to produce mechanically high performant connections due to a matrix blending by interdiffusion. Since LM-PAEK is part of the PEK family, the general

* Degradation onset derived from Thermogravimetric Analysis (TGA).
† Predominant thermal degradation at temperatures above 440°C. Data derived from Polyarlyetheretherkethone (PEEK) composites, considered to be in analogy with LM-PAEK.

findings of Smiley et al. seem to be transferable. Karrasch [22] investigated the relationship between process, interphase morphology and mechanical performance of PEEK/PEI and LM-PAEK/PEI matrix hybrid CFRP`s. Compiling the findings, a difference in the resulting hybrid morphology was observed with respect to local matrix concentration density. But, the LM-PAEK/PEI hot-pressed laminates showed a promising mechanical performance of +17.6 % in G_1C, +5.6 % in SLS whilst -5.4 % in ILSS testing as compared to the PEEK/PEI stacking. However, it has also been shown that temperatures of above 340 °C are necessary to allow for a sufficient miscibility of the LM-PAEK and PEI matrices.

A possible solution to reduce thermal stress during joining of matrix-hybrid components might be given by an out of autoclave Assembly InterDiffusion Joining (AIDJ) process, aligned to conservative Film InterDiffusion Joining (FIDJ) [23]. Introducing the differences of locally heating and pressurizing the respective joining zone by a reduced order joining infrastructure, AIDJ is seen as scalable, energetic preferential and performant alternative as compared to the conventional in oven/ autoclave secondary bonding technique. To investigate the capabilities of the respective matrix combinations and possibilities introduced by the AIDJ process a number of different test specimen were manufactured within the HERFUSE project. Tests are designed to preferentially feed information about the mechanical performance and visualize challenges within non-destructive testing (NDT) of matrix-hybrid structures.

3. EXPERIMENTAL WORK AND CAPABILITY SCREENING

3.1 Coupon Manufacturing

3.1.1 Laminate Configuration A (LC_A):

To evaluate the interphase formation and mechanical performance of the HexPly® 8552/ Ultem™ 1000B laminate configuration (LC_A), coupons were manufactured with a symmetrical stacking sequence, reading $(0°_{15}/\underline{PEI})_S$. As HexPly® 8552 TSC an off the shelf UD prepreg was used with 33 % resin content (RC) by weight, fiber aerial weight of 134 g/m² and IM7 (12k) carbon fibers. Ultem™ 1000B in a thickness of 125 µm, was chosen as thermoplastic PEI film and placed as single layer within the symmetry plane. The plate, with a designed thickness of 4.06 mm, thus later allows to investigate the interphase formation, the single lap shear strength (SLS) as well as the apparent interlaminar lap shear strength (ILSS). For curing, the laminates were press-consolidated within a Wickert WKP4400S hot-press, according to the recommended cure cycle for monolithic components [2].



Figure 2 Image of the HexPly® 8552 stacking with a local integrated Ultem™ 1000B film (left) and closed picture-frame cavity for hotpress consolidation and curing (right).

3.1.2 Laminate Configuration B (LC_B):

TP matrix blending and the mechanical performance of the Cetex® TC1225/ Ultem™ 1000B laminate configuration was evaluated, based on a crossply laminate. An as procured Cetex® TC1225 consolidated plate of Carbon UD T700/LM-PAEK, fiber aerial weight of 145 g/m² and a stacking sequence of $(0°/90°/0°/90°/0°/90°/0°)_s$ was taken to manufacture the residual test laminate in the configuration reading $((0°/90°/0°/90°/0°/90°/0°)_s/\underline{PEI})_s$. Though, a theoretical overall laminate thickness of 4,05 mm was designed, which again allows to conduct the screening tests. The consolidation of the LC_B was performed using the same manufacturing infrastructure and employed according to the recommended static press baseline consolidation cycle for Cetex® TC1225, provided by the National Center for Advanced Materials Performance (NCAMP) [4].

3.1.3 Laminate Configuration C (LC_C):

For LC_C a complex matrix-hybrid composite was manufactured from Cetex® TC1225 (a), Ultem™ 1000B (b), HexPly® 8552S (c) and HexPly® 8552 UD (d). Here, the matrix-hybrid configuration was aligned according to the frame-skin connection but stacked in correlation to the test request and testing standards. The stacking sequence of the resulting laminate reads as follows $((0°)^a{}_{15}/(0°)^b/(0°)^c/(0°)^b/(0°)^d{}_{14})$ and has been stepwise manufactured. In a first step, the pseudo TS skin laminate $((0°)^a{}_{15}/(0°)^b)$ and corresponding TP frame laminate $((0°)^b/(0°)^d{}_{14})$ were manufactured according to the respective processing guidelines (c.f. sections 3.1.1 and 3.1.2). In a second step, the resulting laminate was stacked integrating the HexPly® 8552S coupling layer and cured according to the recommended cure cycle for monolithic components [2]. This stepwise processing procedure reads comparable as for later skin manufacturing, thermoforming of the frames and joining by the AIDJ process.

3. 2 Water-Coupled Ultrasonic Inspection

The manufactured laminates were tested by means of water-coupled ultrasonic testing (WCUT) to check for non-conformance indications, prior to coupon preparation. WCUT was performed using an OLYMPUS OmniScan® SX phased array flaw detector with 5L64-NW1 probe and SNW1-OL-IHC wedge. Probe and wedge were mounted on a 2-axis encoding GLIDER scanner to allow for precise raster scanning. WCUT scans were evaluated using the DLR in-house developed tool Omniscan Plotter. The tool allows to investigate the ultrasonic scans and to apply a certain non-conformance threshold – here -6.0206 dB – with later visualization of possible indications (c.f. Figure 3).

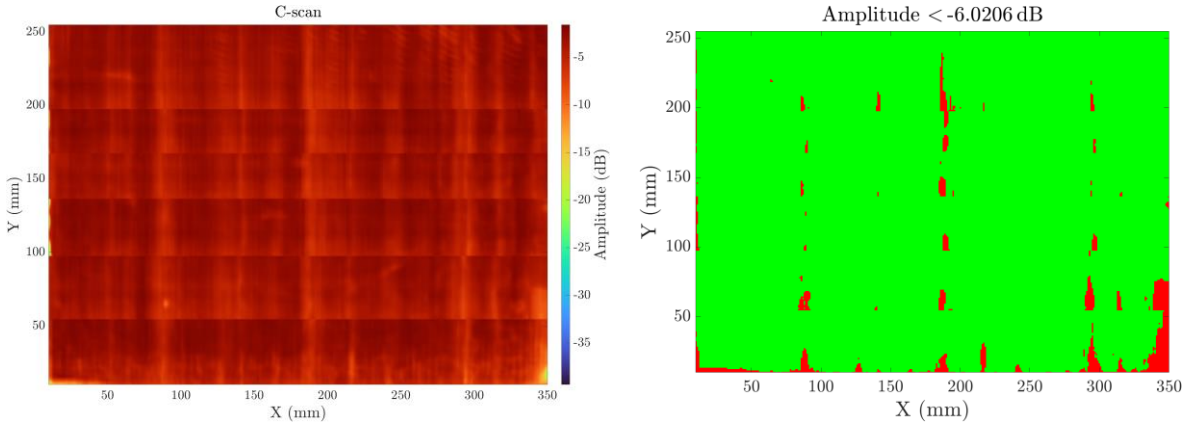


Figure 3 C-Scan of the manufactured LC_A laminate (left) and evaluation plot derived from the Omniscan Plotter with applied -6 dB criterion.

Red marked regions within Figure 3 indicate areas with amplitudes less than this fraction of the reference amplitude as flaws. However, the conducted A- and B-Scan analysis of regions with NDT indications throughout did not show signs of internal laminate defects. LC_A showed a flaw area of 3.09 %. Correlating the indication pattern with the caul plate surface roughness (c.f. Figure 2, right) allows for the conclusion that the imprints are due to the transfer of the milling structure and attributed to increased damping losses at the frontwall echo.

LC_B laminates were accordingly checked for non-conformance indications by means of WCUT. Here, the C-Scan and evaluation results provided a majorly perfect laminate quality with some minor flaws towards the laminate upper cutting edge, resulting in an overall flaw area of 0.21 %. A validation of the A-Scan as well the B-Scans in X- and Y-direction offers a reduced backwall echo in between ($224.5 \leq X \leq 301.3$) over a width of 2.3 mm, but no obvious interruption of the stacking such as delamination. NDT of the LC_C hybrid plate showed a majorly consistent high-quality laminate. Increased damping losses were recorded towards the surrounding cutting edges, leading to a flaw area of 8.87 %. Here, the flaw area showed in comparison to regions without non-conformance indications a shift of the backwall echo towards a reduced laminate thickness. The location of the defects suggests that increased matrix bleed-out occurred at the edges of the plates due to the manufacturing process used in combination with the shape of the mold. Following, reflected-light microscopical investigations were employed in order to deeper investigate the root cause of the increased acoustic damping losses (c.f. section 3.3.3).

3.3 Destructive Testing

3.3.1 Slotted Single Lap Shear Strength

To check for the mechanical performance of the matrix-hybrid laminates, two destructive testing (DT) methods were employed. First, tensile lap shear strength was determined according to AITM1-0019, based on five extracted slotted SLS specimens. All SLS tests were performed at room temperature (RT) on a Shimadzu AGX-V2 300 kN tensile testing machine, as received (AR) without prior coupon conditioning. Resulting in a determined SLS strength of (15.4 ± 0.7) MPa, the coupons of LC_A entirely showed a failure due to delamination within the HexPly® 8552 adherent, suggesting an adequate interdiffusion between the 8552 and PEI matrices with preferential toughness modification. In comparison, Palmieri reported from SLS strength values of (16.4 ± 0.6) MPa [24] for a pristine HexPly® 8552 laminate thus being 6 % higher as compared to the as manufactured LC_A laminate.

Same for LC_B, the test coupons were extracted from the flawless regions of the respective laminates. Here, DT of the slotted SLS coupons resulted in a tensile lap shear strength of (33.5 ± 2.9) MPa. The fracture surfaces consistently exhibited cohesive failure adjacent to the adherent, which is attributable to the combined shear and peel stresses acting on the SLS test specimens. In comparison, a manufactured Cetex® TC1225 reference laminate of the same stacking sequence without PEI layer led to SLS values within the same magnitude being (33.2 ± 2.5) MPa. The results offer that the maximum achievable SLS values are quite underestimated and decreased by the introduced peel load. However, as described by Villegas, SLS testing is a valuable and flexible tool for comparison and/ or addition to further tests for gaining insights into the mechanical properties of polymer composites [25]. Testing results of LC_C provided a tensile lap shear strength of (20.2 ± 2.9) MPa with mixed failure due to delamination within the HexPly® 8552 UD (d) component and partly delamination of the

HexPly® 8552S (c) coupling layer. From the SLS strength values and a visual inspection of the fracture surfaces it was concluded, that the material choice and applied AIDJ joining principle leads to a sufficient structural connection between the investigated matrices. Here, the increased SLS values of +31.2 % as compared to LC_A are attributed to a preferential toughness modification through the PEI surface modification of the components.

Table 2 Overview of the SLS strength values achieved in relation to the corresponding laminate configuration and comparative reference values.

	LC_A	HexPly® 8552_REF	LC_B	Cetex® TC1225_REF	LC_C
SLS [MPa]	15.4 ± 0.7	16.4 ± 0.6 [24]	33.5 ± 2.9	33.2 ± 2.5	20.2 ± 2.9

3.3.2 Apparent Interlaminar Shear Strength

As second DT method, the apparent interlaminar shear strength (ILSS) was investigated by means of six test coupons at RT/AR. The tests were performed according to ISO 19927 on a 5-point-bending fixture within an MTS Criterion C45.105 testing machine. From coupons of LC_A, ILSS values of (142.5 ± 4.0) MPa are measured. All tested specimen showed an acceptable failure due to delamination with slight independent local crushing. In comparison, the manufacturer's technical datasheet offers a slightly reduced ILSS baseline value of 137 MPa for the pristine HexPly® 8552, tested at RT in dry condition [2]. From LC_B, ILSS values of (117.6 ± 3.9) MPa are derived. Predominantly failure due to a shear band with delamination was observed, which is described as unacceptable according to the standard. However, introducing the PEI film increases the ILSS values at 21.9 % when comparing to the pristine Cetex® TC1225 [3]. The testing results of LC_C provided ILSS values of (124.0 ± 6.8) MPa and an according to the standard acceptable failure due to delamination with slight independent local crushing. In comparison to the residual tests this means a reduction of 13.0 % as compared to LC_A and an increase of 5.4 % as compared to LC_B.

Table 3 Overview of the ILSS values achieved in relation to the corresponding laminate configuration and comparative reference values.

	LC_A	HexPly® 8552_REF	LC_B	Cetex® TC1225_REF	LC_C
ILSS [MPa]	142.5 ± 4.0	137 [2]	117.6 ± 3.9	96.5 [3]	124.0 ± 6.8

3.3.3 Interphase Characteristics

To gather additional insight into the interphase formation and interlocking mechanisms, reflected-light microscopical investigations were employed using a Keyence VHX-5000 digital microscope with VH-Z250R zoom lens. Selected specimens were grinded by a Struers LaboPol - 30 automatic grinder and accordingly polished using a diamond suspension (9 – 3) µm. Following, specimens were examined with (w/) and without (w/o) prior Dichloromethane (DCM) etching at 250-fold and 500-fold magnification, respectively. A visual comparison of the images taken of the interphase from the LC_A depicts an undisturbed composite without visual indications for an inadequate matrix interdiffusion (c.f. Figure 4). At the left-hand side microscopic image w/o DCM etching a different contrast of the respective matrices can be observed showing the 8552 matrix a slight magnitude darker as compared to the PEI film. However, it can be observed that the residual PEI thickness remains approximately on its initial thickness of 125 µm generating a slim interdiffusion zone.

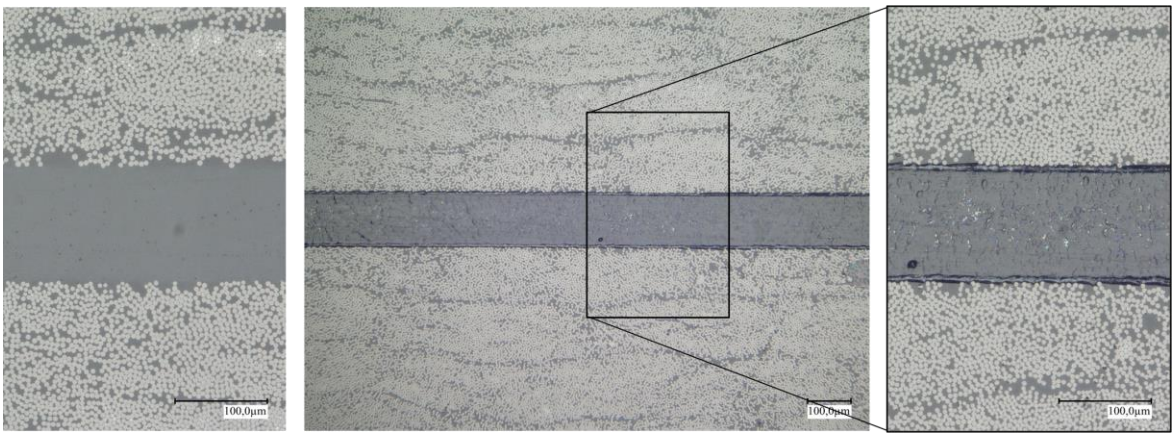


Figure 4 Reflected-light microscopical images taken from representative locations w/o (left) and w/ (middle & right) DCM etching of LC_A at 250-fold and 500-fold magnification.

Microscopical images taken from the LC_B (Figure 5) illustrate a visually adequate polymer blending of the TP matrices and fiber migration from TC1225 into the neat PEI layer. Again, no visual boundary as indication for a weak connection can be observed from the microscopic images, but from the etched specimen matrix interlocking becomes visually clear.

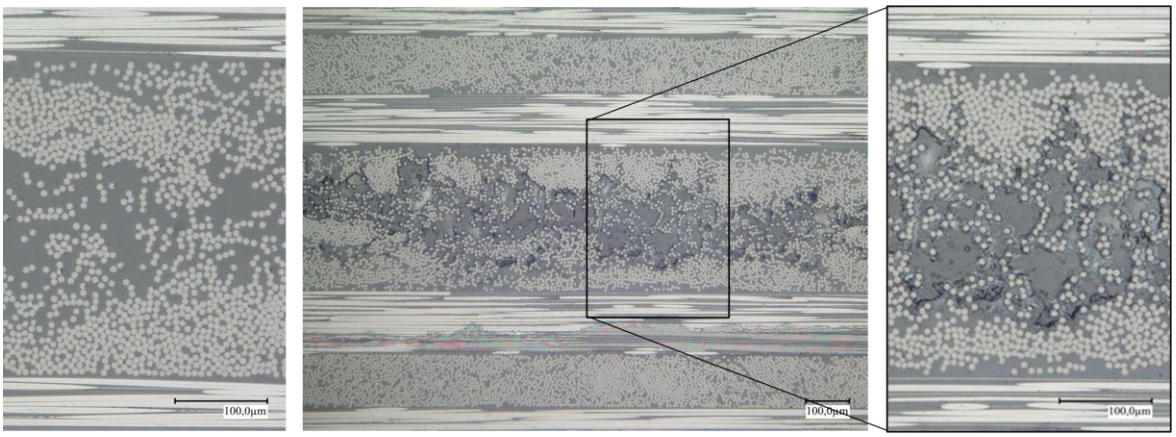


Figure 5 Reflected-light microscopical images taken from representative locations without (left) and with (middle & right) DCM etching of LC_B at 250-fold and 500-fold magnification.

Figure 6 being images taken from the LC_C, depicts comparable findings as concluded from LC_A and LC_B, with no visible indication for matrix interruption or weak connection. Same as for LC_B, fiber migration from TC1225 into the neat PEI layer can be observed. Over the entire cross-section slight porosity becomes visible, especially accumulated in regions where the fabrics rovings cross at warp and weft and forming a cavity. Measuring the cure ply thickness of the HexPly® 8552S (c) coupling layer (252.2 ± 3.8) µm within the matrix-hybrid laminate yields a reduction of 12.7 % as compared to the nominal cure ply thickness of 289 µm. Thus, the observed porosity was attributed to an increased lateral matrix bleed out.

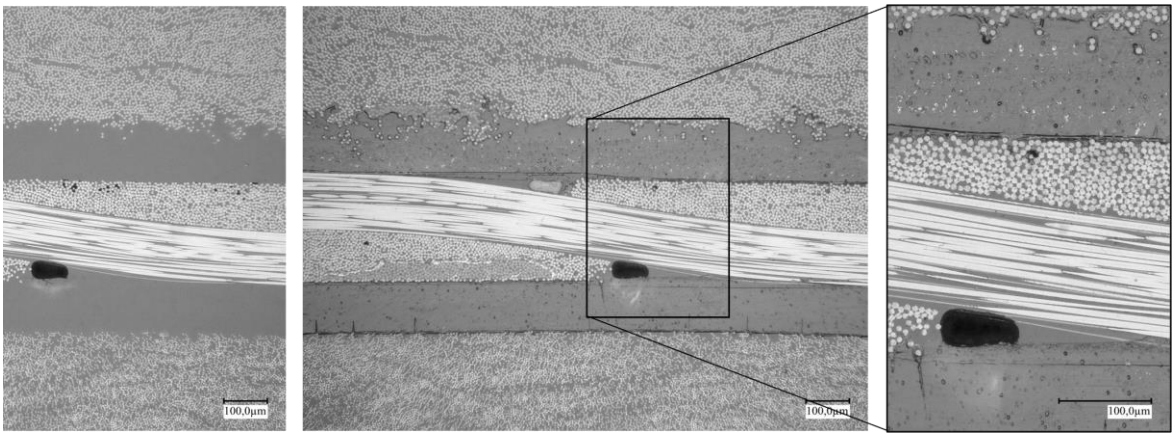


Figure 6 Reflected-light microscopical images taken from representative locations without (left) and with (middle & right) DCM etching of LC$_C$ at 250-fold and 500-fold magnification.

5. CONCLUSION AND WAY FORWARD

The present publication allows a glimpse around the activities for joining of the hybrid lateral panel, within the HERFUSE project. A reduced order capability screening program is presented, elaborating challenges and opportunities for joining HexPly® 8552 thermoset- and Cetex® TC1225 thermoplastic components. It is focussed on highlighting the differences in processing requirements within single part manufacturing of the respective TS and TP components, whilst discussing hurdles on applying conventional thermoplastic fusion bonding technologies. Local blending of the single components for surface modification with an amorphous Ultem™ 1000B PEI film introduces the opportunity to conduct a following applied interdiffusion-based joining process.

Three different CFRP laminate configurations have been manufactured and tested in order to visualize possible hurdles in non-destructive testing and elaborate the mechanical performance by means of SLS and ILSS testing. Microscopic examinations of cross-section samples are conducted to gain a deeper understanding for the interphase development and find correlations with respect to NDT non-conformance indications. First laminate, manufactured from HexPly® 8552/ Ultem™ 1000B was defined to being representative for the local surface modification of the demonstrator's skin laminate. The second configuration of Cetex® TC1225/ Ultem™ 1000B should gain deeper understanding on the necessary blending of the later frame outer-surface. Third, a complex matrix-hybrid composite laminate was manufactured and tested, being representative for the overall combination of frame, coupling layer and skin. The as manufactured laminates within this capability screening were consistently manufactured within a hot-press.

For the lateral panel joining process a reduced-order infrastructure is developed, yielding the basic boundary conditions comparable to a hot-press. Thus, it is expected that the basic findings from laminate manufacturing are transferable towards full-scale manufacturing and joining of the HERFUSE matrix-hybrid lateral panel. In parallel, a comprehensive testing campaign is conducted as part of the project, providing deeper insight related to the challenges and opportunities introduced by the AIDJ process.

Acknowledgments

This project has received funding from the Clean Aviation Joint Undertaking (CAJU) under grant agreement No 101140567. The JU receives support from the European Union's Horizon 2020 research and innovation program.

Disclaimer

Views and opinions expressed are however those of the author(s) only and do not necessarily reflect those of the European Union or Clean Aviation Joint Undertaking. Neither the European Union nor Clean Aviation JU can be held responsible for them.





5. REFERENCES

[1] Y.C. Roth, R. Herrmann, C. Sanchez Santos, M. Uellendahl, J. Koopman, A. Henneberg, J. Kos, I.F. Villegas, A. Choudhary, L. Larsen, S. Ferstl, B. Diehl, F. Emanuelsson, J.-B. Sinéchal, M. Pleth, and K. Atherton, "CleanSky2/ Clean Aviation Large Passenger Aircraft For More Sustainable Commercial Fuselage Technologies - Major Achievements," *34th Congress of the International Council of the Aeronautical Sciences, ICAS 2024*, 2024.

[2] H. Corporation, "HexPly® 8552 Epoxy matrix (180°C/356°F curing matrix)," 2023.

[3] T.A. Composites, "Toray Cetex® TC1225 LM-PAEK™ Product Data Sheet," 2025.

[4] R. Lovingfoss, R. Andrulonis, V. Tanoto, and J. Tomblin, *NCAMP Process Specification Fabrication of NMS 122 Qualification, Equivalency, and Acceptance Test Panels, Medium Toughness Polyaryletherketone (PAEK) Thermoplastics Toray (Formerly TenCate) Cetex® TC1225 Low Melt (LM) Polyaryletherketone (PAEK)*, Wichita State University, National Institute for Aviation Research, 2025.

[5] M. Abouhamzeh and J. Sinke, "Effects of fusion bonding on the thermoset composite," *Composites Part A-applied Science and Manufacturing*, 2019.

[6] M. Day, J.D. Cooney, and D.M. Wiles, "The kinetics of the oxidattve degradation of poly(aryl-ether-ether-ketone) (PEEK)," *Thermochimica Acta*, vol. 147, Jul. 1989, pp. 189–197.

[7] A. Sänger, "Ein Qualitätsfaktor beim Schweißen thermoplastischer Faserverbunde mittels Meso-Composite-Modell," Universität Augsburg, 2024.

[8] R.L. Evelyn Lian and V. Tanoto, *Medium Toughness PAEK thermoplastics Toray (Formerly TenCate) Cetex® TC1225 (LM PAEK) T700GC 12K T1E Unidirectional Tape 145 gsm 34% RC Qualification Material Property Data Report*, National Institute for Aviation Research Wichita State University 1845 N. Fairmount Wichita, KS 67260-0093: Wichita State University, National Institute for Aviation Research, 2020.

[9] Sabic, "ULTEM™ 1000B Film - Product Datasheet," 2020.

[10] T. Karrasch, "Entwicklung eines Schweißprozesses zum Fügen eines oberflächenmodifizierten Duromerbauteils mit einem Thermoplastbauteil (Masterarbeit)," Hochschule Augsburg, 2019.

[11] C. Ageorges and L. Ye, "Resistance welding of thermosetting composite/thermoplastic composite joints," *Composites Part A-applied Science and Manufacturing*, 2001.

[12] L. Vandi, M. Hou, M. Veidt, R.W. Truss, M. Heitzmann, and R. Paton, "Interface diffusion and morphology of aerospace grade epoxy co-cured with thermoplastic polymers," *null*, 2012.

[13] M.T. Heitzmann, M. Hou, M. Veidt, L. Vandi, and R. Paton, "Morphology of an Interface between Polyetherimide and Epoxy Prepreg," *Advanced Materials Research*, 2011.

[14] I.F. Villegas and R. van Moorleghem, "Ultrasonic welding of carbon/epoxy and carbon/PEEK composites through a PEI thermoplastic coupling layer," *Composites Part A-applied Science and Manufacturing*, 2018.

[15] T. Maierhofer, E.G. Loukaides, C. Carr, C. Bisagni, and R. Butler, “Resistance-welded thermoset composites: A Bayesian approach to process optimisation for improved fracture toughness,” *Composites. Part A, Applied science and manufacturing*, 2023.

[16] R. van Moorleghem, “Welding of thermoplastic to thermoset composites through a thermoplastic interlayer,” Technische Universität Delft, 2016.

[17] P. Bruckbauer, “Struktur-Eigenschafts-Beziehungen von Interphasen zwischen Epoxidharz und thermoplastischen Funktionsschichten für Faserverbundwerkstoffe,” 2018.

[18] T. Maierhofer, E. Loukaides, T. Hernandez, C. Carrc, C. Bisagnid, and R. Butlera, “fracture toughness and performance of resistance-welded and co-bounded thermoset/thermoplastic polymer composite hybrid joints,” *Composites Meet Sustainability – Proceedings of the 20th European Conference on Composite Materials*, vol. 2, Jun. 2022.

[19] M. Bois, “Mechanical properties of Thermoplastic/Thermoset interphases,” Université catholique de Louvain, 2016.

[20] I.F. Villegas and P.V. Rubio, “On avoiding thermal degradation during welding of high-performance thermoplastic composites to thermoset composites,” *Composites Part A: Applied Science and Manufacturing*, vol. 77, 2015, pp. 172–180.

[21] A. Smiley, A. Halbritter, F. Cogswell, and P. Meakin, “Dual Polymer Bonding Of Thermoplastic Composite Structures,” *Polymer Engineering and Science*, 1991.

[22] T. Karrasch, “Charakterisierung der Prozess-Morphologie-Eigenschaftsbeziehungen von hybriden Thermoplast-Thermoplast Interphasen im Hinblick auf Thermoplast-Duromer Hybride für Luftfahrtanwendungen,” Universitä, 2024.

[23] M. Endrass, C. Schmidt-Eisenlohr, A. Buchheim, and A. Cords, “Neue Verbindungstechnologien für duromere Faserverbundkunststoffe: Eine Alternative zu konventionellen Bolzenverbindungen,” *Deutsche Gesellschaft für Luft- und Raumfahrt - Lilienthal-Oberth e.V.*, AmTechnologiezentrum 4, 86159 Augsburg, Deutschland: Deutsches Zentrum für Luft- und Raumfahrt (DLR), Zentrum für Leichtbauproduktionstechnologie (ZLP), 2025.

[24] F. Palmieri, T. Hudson, R. Cano, E. Tastepe, D. Rufeisen, L. Ahmed, yi Lin, C. Wohl, and J. Connell, “Reliable Bonding of Composite Laminates Using Reflowable Epoxy Resins,” *SAMPE 2019 - Charlotte, NC*, SAMPE, 2019.

[25] I.F. Villegas and C. Rans, “The dangers of single-lap shear testing in understanding polymer composite welded joints,” *Philosophical Transactions of the Royal Society A: Mathematical, Physical and Engineering Sciences*, vol. 379, Jun. 2021, p. 20200296.